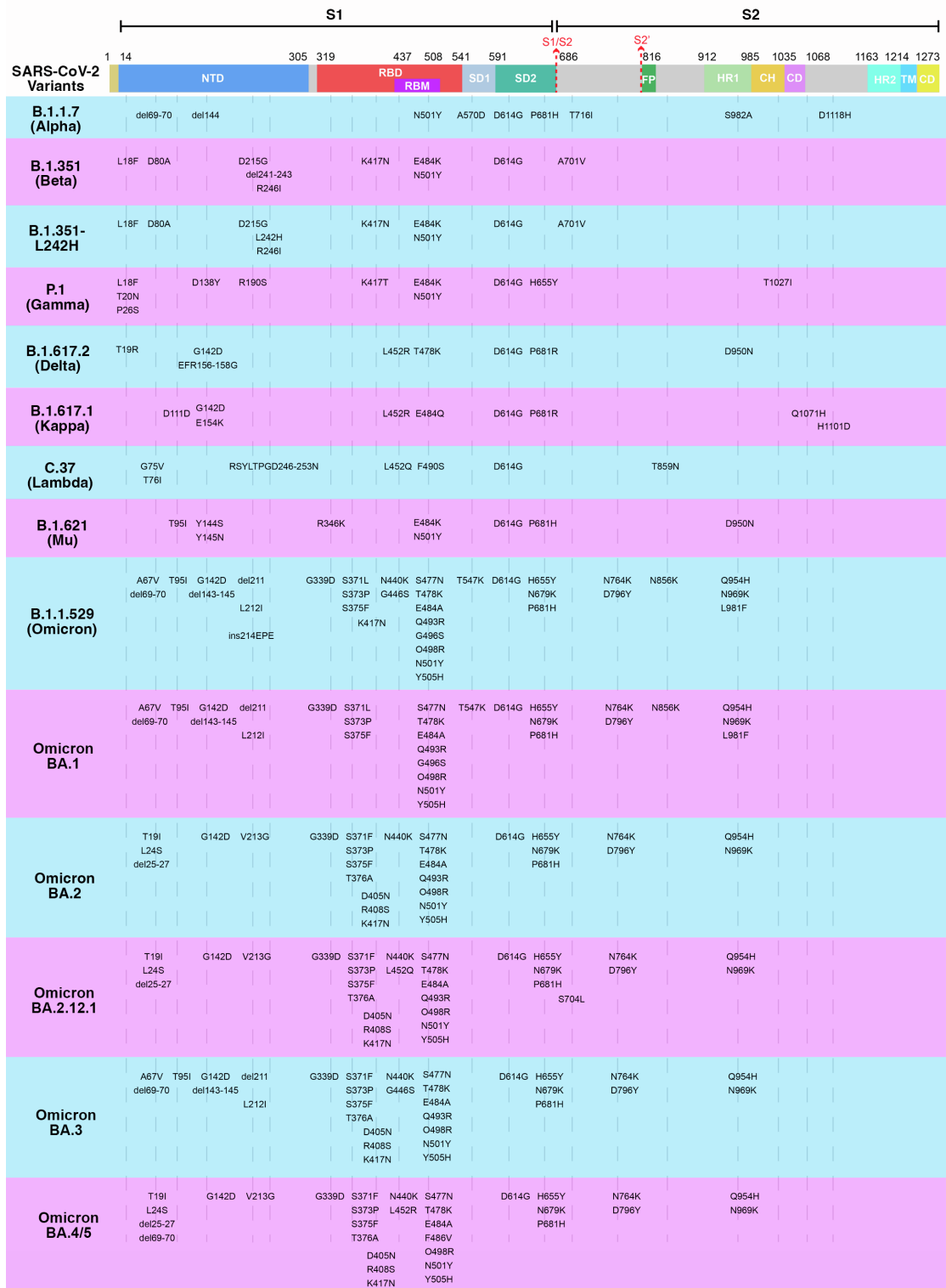


**Supplemental information**

**Fortuitous somatic mutations during antibody  
evolution endow broad neutralization  
against SARS-CoV-2 Omicron variants**

Jianbo Wu, Zhenguo Chen, Yidan Gao, Zegen Wang, Jiarong Wang, Bing-Yu Chiang, Yunjiao Zhou, Yuru Han, Wuqiang Zhan, Minxiang Xie, Weiyu Jiang, Xiang Zhang, Aihua Hao, Anqi Xia, Jiaying He, Song Xue, Christian T. Mayer, Fan Wu, Bin Wang, Lunan Zhang, Lei Sun, and Qiao Wang

## SUPPLEMENTARY FIGURES AND LEGENDS



**Figure S1. S protein mutations within SARS-CoV-2 variants. Related to Figure 1.**

Key spike mutations found in the SARS-CoV-2 variants, compared with Wuhan-Hu-1 (wild-type), are denoted. These variants include five SARS-CoV-2 VOCs: B.1.1.7 (Alpha), B.1.351 (Beta), P.1 (Gamma), B.1.617.2 (Delta) and B.1.1.529 (Omicron); five Omicron variants: BA.1, BA.2, BA.2.12.1, BA.3 and BA.4/5; and four other variants: B.1.351-L242H, B.1.617.1 (Kappa), C.37 (Lambda) and B.1.621 (Mu).

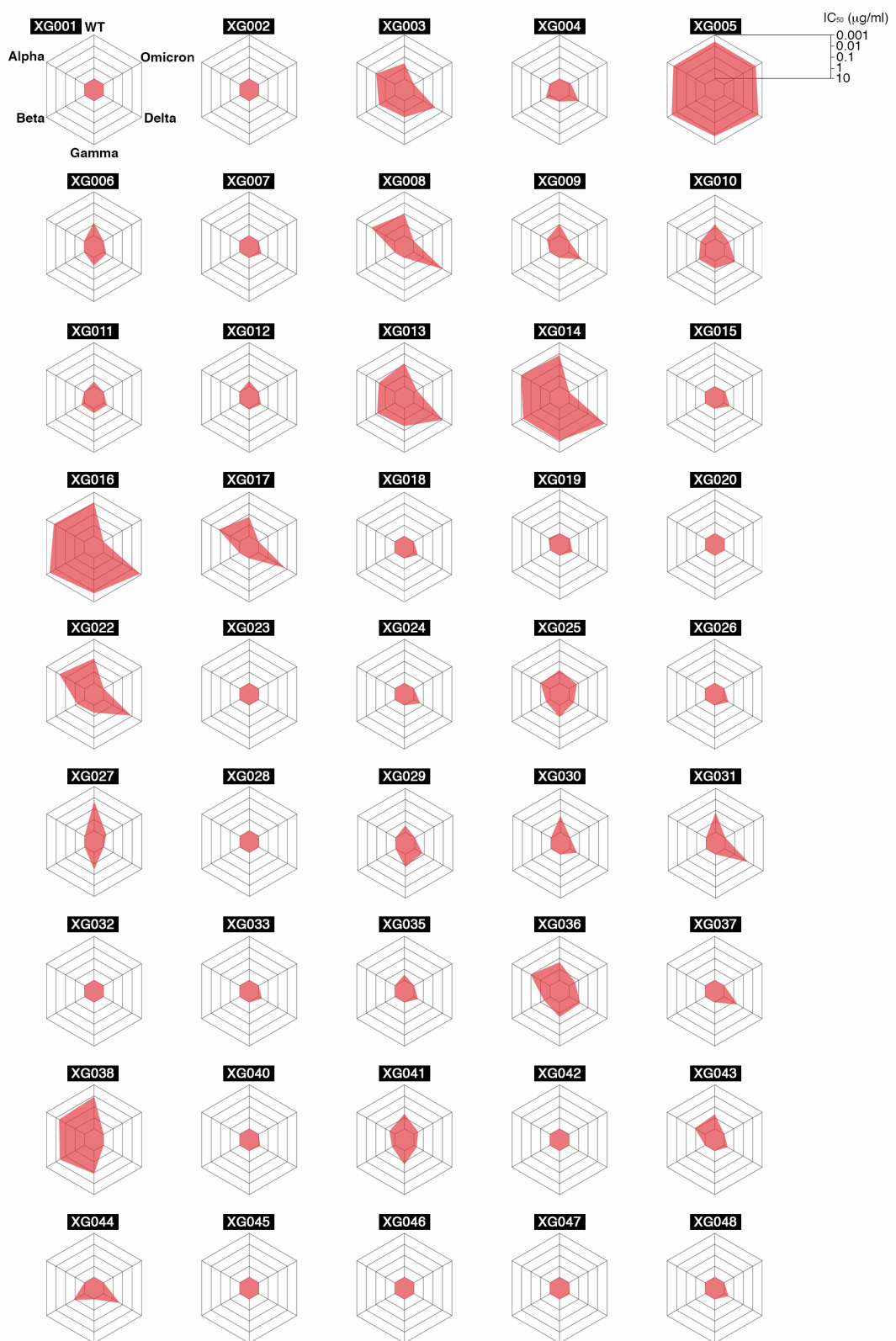


**Figure S2. Spider charts for  $IC_{50}$  values of 45 mAbs. Related to Figure 2.**

$IC_{50}$  values against Wuhan-Hu-1 (wild-type), B.1.1.7 (Alpha), B.1.351 (Beta), P.1 (Gamma), B.1.617.2 (Delta) and B.1.1.529 (Omicron) pseudoviruses were measured for all 45 tested antibodies isolated from a convalescent donor ([Zhou et al., 2021](#)).

Antibodies with  $IC_{50}$  values (mean of two independent experiments.) above 10  $\mu\text{g}/\text{ml}$  were shown as 10  $\mu\text{g}/\text{ml}$ .

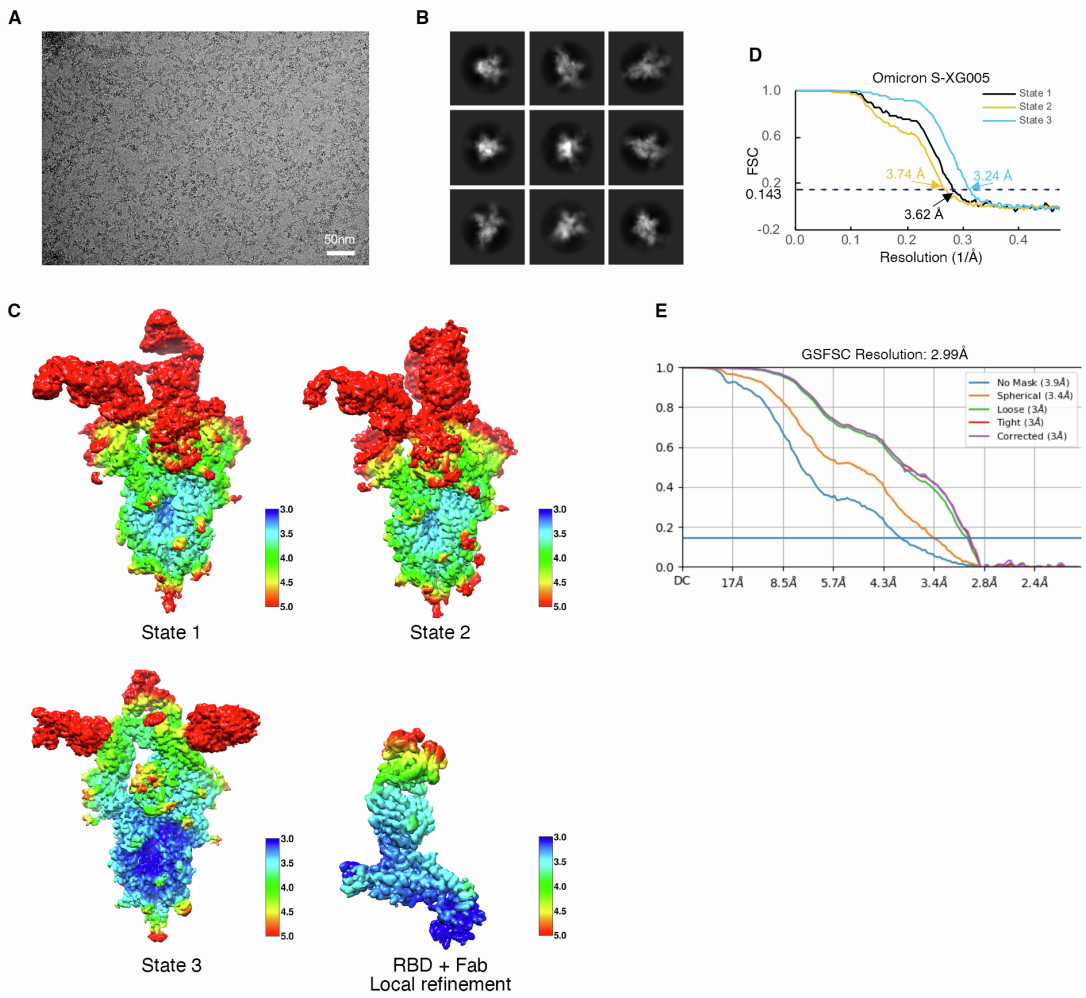


**Figure S3. Cryo-EM data collection and processing of Omicron S-XG005**

**complex (OS-XG005). Related to Figure 3.**

(A) Representative electron micrograph.

(B) 2D classification results of OS-XG005.

(C) Local resolution of the reconstruction maps generated by DeepEMhancer.

(D) Gold-standard Fourier shell correlation curves (FSC) for each structure. The 0.143 cut-off is indicated by a horizontal dashed line.

(E) FSC of local refinement of RBD-XG005 Fab region obtained from cryoSPARC.

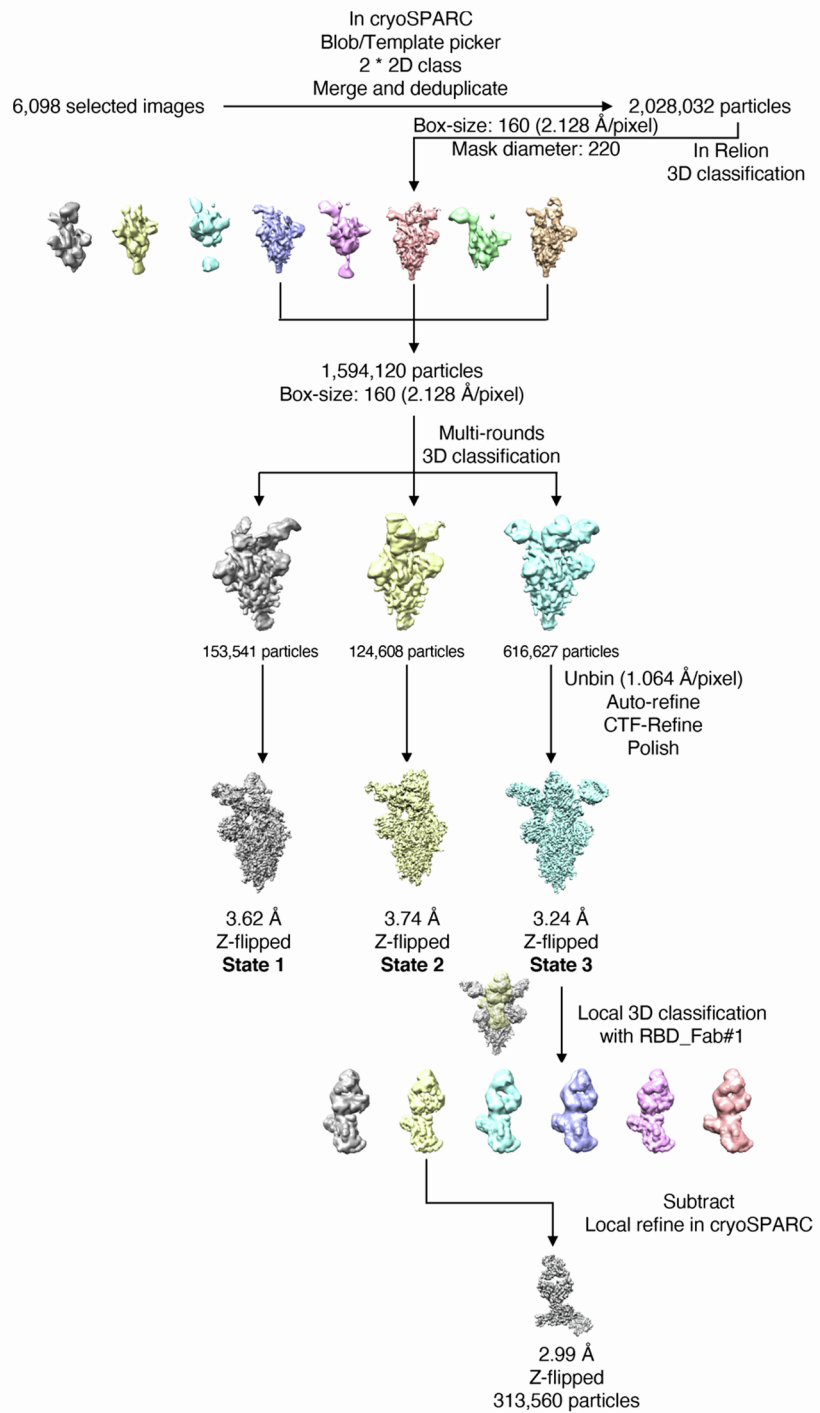


**Figure S4. Data processing flowchart of OS-XG005 complex. Related to Figure 3.**

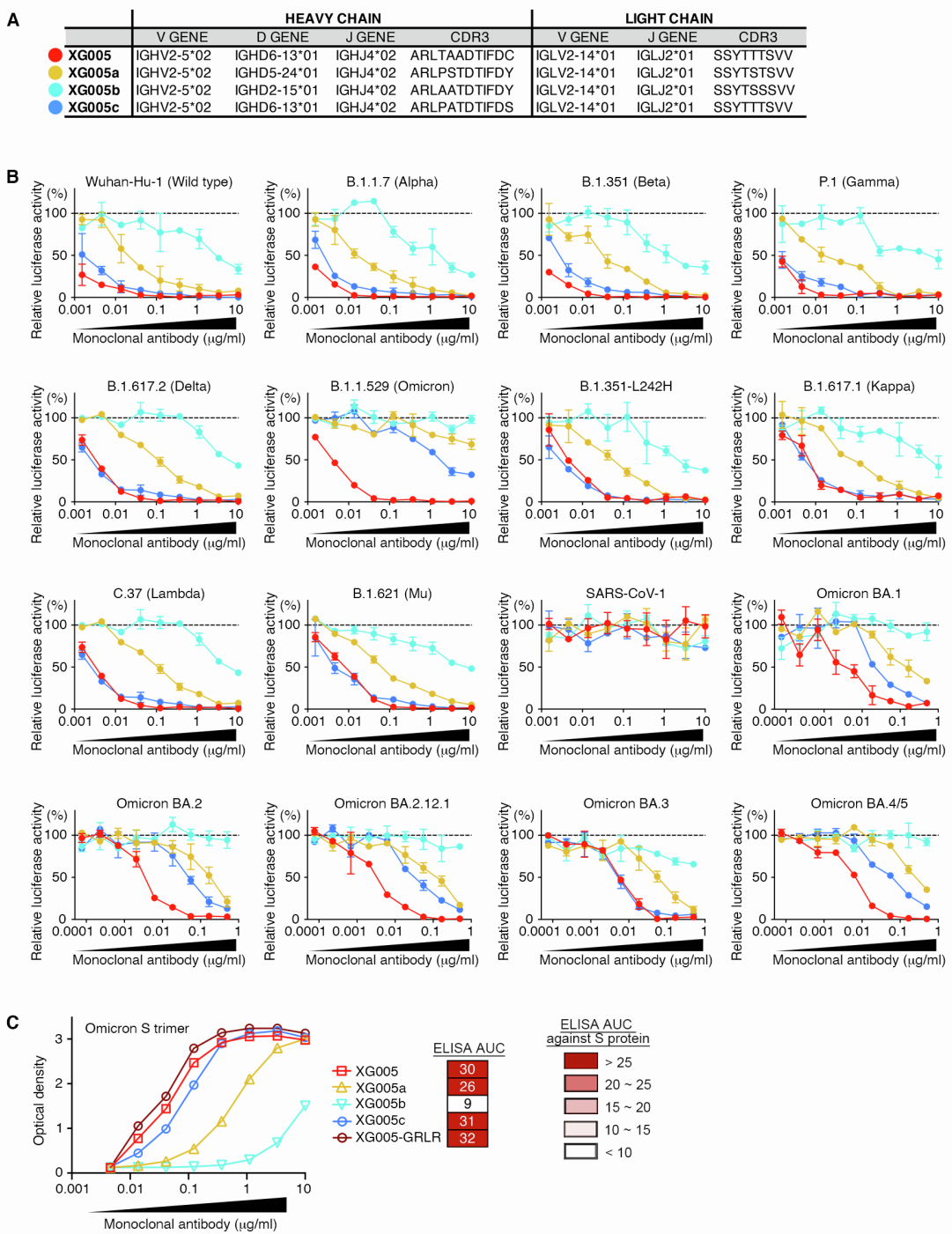


**Figure S5. In vitro pseudovirus neutralization assays for XG005 family members. Related to Figure 5.**

(A) V(D)J assignments for the XG005 clone. IMGT/V-QUEST was used to assign the V, D, J genes and CDR3 sequences for their Ig heavy and light chains.

(B) Neutralization potency of XG005 family members. Luciferase-based pseudoviruses were used for in vitro infection. Dashed line represents no antibody control. All experiments were repeated at least twice, presented as mean ± SEM.

(C) Dramatically distinct binding capacity against Omicron S protein by XG005 family members. ELISA assays to determine the antibody binding capacity against Omicron S proteins. ELISA area under the curve (AUC) values were calculated. XG005c showed similar level of binding activity of XG005, while those of XG005b and XG005c dramatically reduced.

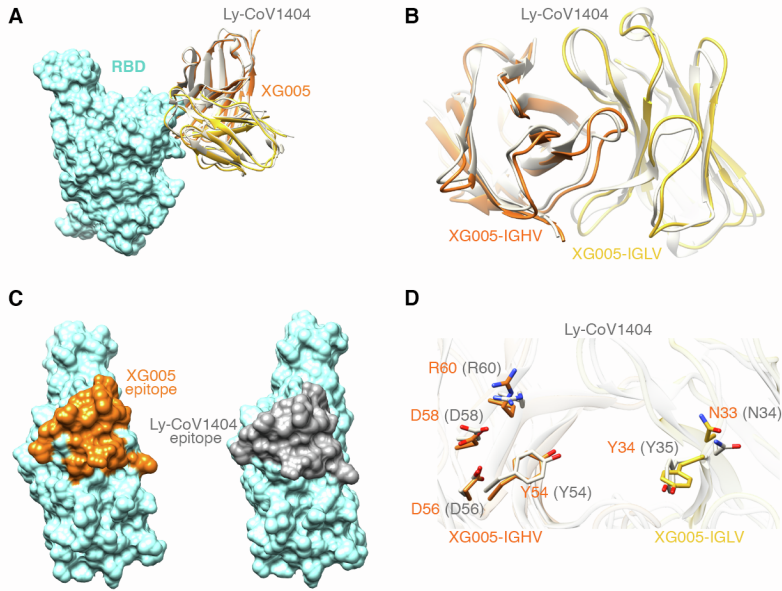


**Figure S6. Structural comparison between XG005 and LY-CoV1404. Related to Figure 5.**

(A) Comparison the models of wild-type RBD complexed with XG005 and LY-CoV1404. RBD is displayed in sky-blue surface; XG005 heavy and light chains are shown in orange and yellow ribbons, respectively, while LY-CoV1404 is shown in gray.

(B) A close view of XG005 and LY-CoV1404.

(C) Surface representation of RBD showing the interfaces of XG005 (orange) and LY-CoV1404 (dark gray), respectively.

(D) Comparison of the key residues of XG005 and LY-CoV1404 involved in the RBD interaction. Residues of XG005 and LY-CoV1404 are labeled in orange and gray, respectively.

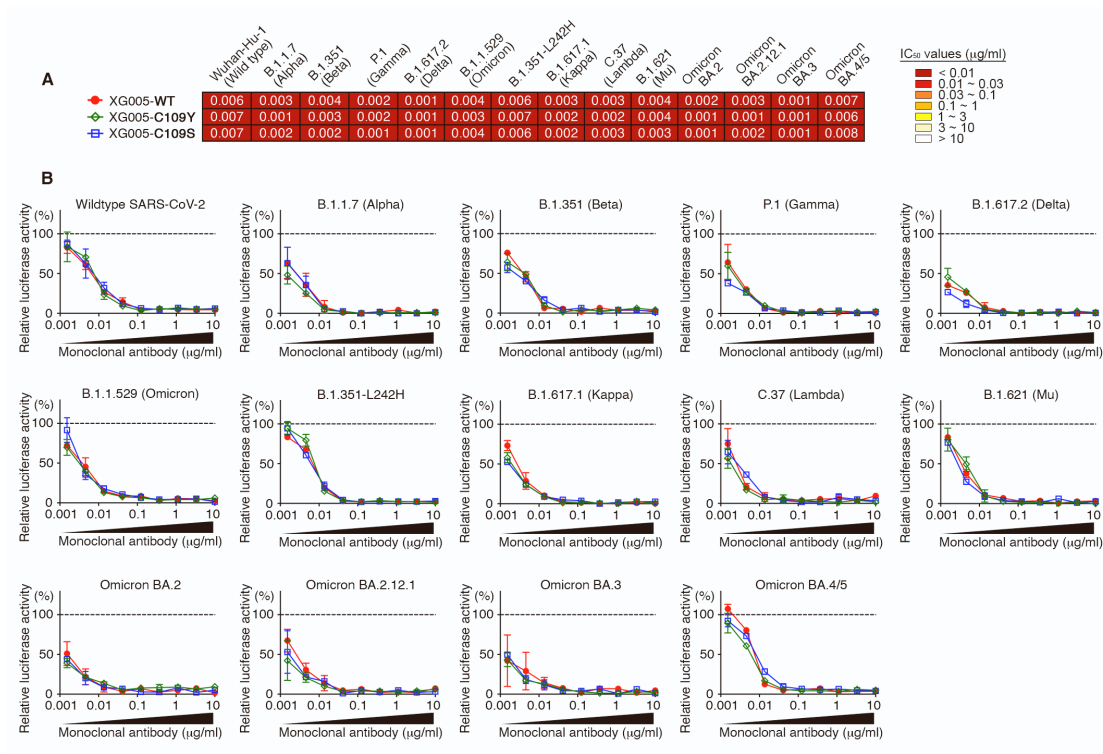


**Figure S7. Engineered C109 variants of XG005 maintain neutralization potency.**

### Related to Figure 7.

(A) IC<sub>50</sub> values for XG005-WT, XG005-C109Y, and XG005-C109S measured

against pseudoviruses of SARS-CoV-1, SARS-CoV-2 and its variants.

(B) Pseudovirus neutralization assays using different concentrations of XG005-WT,

XG005-C109Y, and XG005-C109S. Mean of two independent experiments.

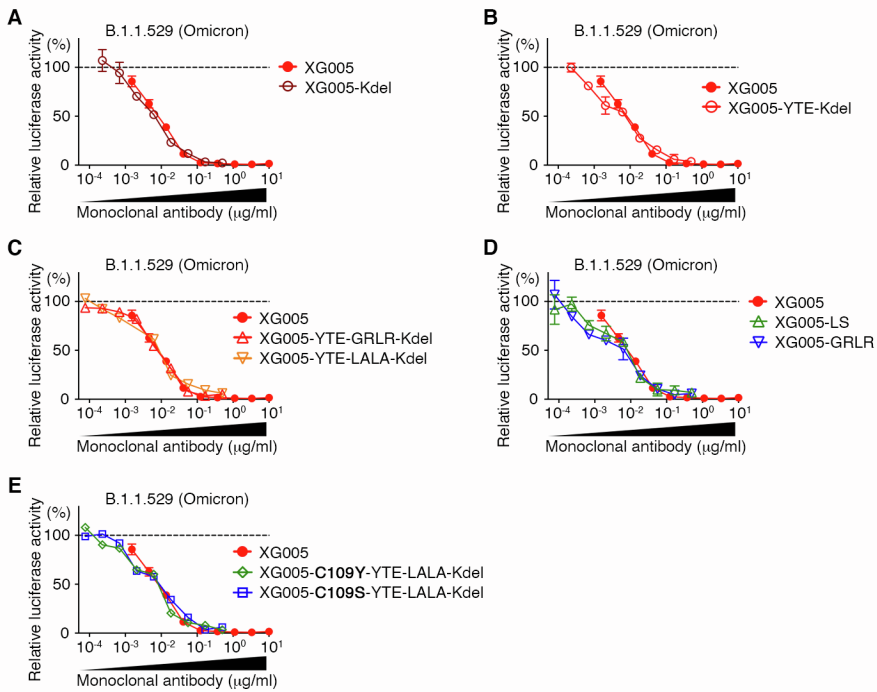


**Figure S8. Engineered Fc variants of XG005 maintain neutralization potency.**

**Related to Figure 7.**

(A-D) Various engineered Fc variants of XG005 maintain the in vitro neutralizing activities against B.1.1.529 (Omicron) pseudoviruses. Kdel: mAb mutant with the deletion of heavy chain C-terminal lysine (A). YTE: mAb mutant with triple mutations M255Y, S257T and T259E in the Fc domain (B and C). LS: mAb mutant with M431L and N437S mutations in the Fc domain (D). Both YTE and LS substitutions result in an increase in its binding to human FcRn and a prolonged serum half-life of the antibody. GRLR: mAb mutant with G239R and L331R mutations in the Fc domain (C and D). LALA: mAb mutant with L237A and L238A mutations in the Fc domain (C). Both GRLR and LALA substitutions abrogate the antibody binding to FcγRs and eliminate the ADE effect.

**Table S1. Cryo-EM data collection and refinement statistics of the Omicron S-XG005 complex. Related to Figure 3.**

	State 1 (UDD with two Fabs)	State 2 (UDD with three Fabs)	State 3 (UDU with three Fabs)	RBD+Fab XG005
<b>Data collection and processing</b>				
Magnification		81,000		
Voltage (kV)		300		
Total dose (e <sup>-</sup> /Å <sup>2</sup> )		58		
Defocus range (μm)		-1.2 to -2.5		
Pixel size (Å)		1.064		
Symmetry imposed		C1		
Final particles (no.)	153,541	124,608	616,627	313,560
Map resolution (Å)	3.62	3.74	3.24	2.99
<b>Refinement</b>				
<b>R.m.s. deviations</b>				
Bond lengths (Å)	0.002	0.002	0.002	0.002
Bond angles (°)	0.558	0.509	0.517	0.479
<b>Validation</b>				
MolProbity score	2.40	2.24	2.23	2.46
Clashscore	7.16	5.99	6.11	6.30
Rotamer outlier (%)	5.83	4.53	4.85	5.46
<b>Ramachandran plot</b>				
Favored (%)	93.64	93.72	94.54	90.05
Allowed (%)	6.36	6.28	5.44	9.95
Disallowed (%)	0.00	0.00	0.00	0.00
<b>EMDB</b>	EMD-33744	EMD-33742	EMD-33743	EMD-33745
<b>PDB</b>	7YD0	7YCY	7YCZ	7YD1

**Table S2. Amino acid sequences of the S protein of various pseudotyped viruses used for in vitro neutralization assays. Related to STAR Methods.**

B.1.617.2 (Delta)	MFVFVLLPLVSSQCVNLRTTQLPAPPNTSFRGVVYYPDKVFRSSVLHSTQDLFLPFFSNVTWFHAIHVGSTNGTKRFDNVPVLPFNDGVYFASTEKSNIIRGWIFGTTLDSKTQSLLIVNNATNVIKVCEFCQFCNDPFLDVYHHKNNKSWMEGVYSSANNCCTFEVSOFPFLMLEGKGQGNFKNLREFVFKNIDGYFKYKSHTPINLVRDLPQGSALEPLVLDLPIGINITRFQTLLAHLHSYLTPOSSCGWITAGAAAAYVGYLQPRFTFLKYNNENGTTDAVDACDPLPSETKCTLSFTVEKGIVYOTSFRVQPTESVRFPNITNLCPGEVFNATRFASVYAWNKRISNCVADYSVLYNSASFSTFKCYGVSDSSCGVPTKLNDLCFTNVYADSFVIRGVDEVRQIAQPGQTCGKSTNLVKNCVNFNGLTGTGVLTESNKKFLPFQGFRDIADTTDAVRDPOTLEIDLITPCSGFGSVVITPGNTTSNOVAVLYQGVNCTEVPAVIAHADOLTPTWRYSTGSNTVQTRAGCLIGAEVNNSYEDIPIGACISYQTQNSRRARSVASQSIAYTMSLGAENSVASNNSIAIPNTFTISVTEILPVSMTTKSVDCTMYICGDSTECNLLOYSGFCTQLNRLALTGIAVEQDKNTQEFAQVKQINCKTPPKDFGGFNSQDLPSPSKRSFIEDLFLNKVTLADAGFKIYQGDCGLDIAARDLICAQKFNGLTVLPPLTDEMIAQYTSALAGITTSQTYTQQLRRAEIRASANLAATKMSCEVLGQSKRVDFCGKGYHLMSPQSAHPGVFLHVTVPAQEKNFTTAPACHDGKAHFREGVVFVSGNTHWFTQRNFYEPQIITTDNTFVSGNCDDVIVNNNTVYDPLQPELDSFKEELDKYFKNHTSPDVLDGDISGINASVNIKEIDRNEAKNLNESLIDLQELGKYEQYIKWPWYIWLGFIAGLIAVMVIMLCMTSCSCLKGCCSCGCKFSCFKFEDDSEPVLKGVKLHY*	T19R, G142D, EFR156-158G, L452R, T478K, D614G, P681R, D950N
C.37 (Lambda)	MFVFVLLPLVSSQCVNLRTTQLPAPPNTSFRGVVYYPDKVFRSSVLHSTQDLFLPFFSNVTWFHAIHVGSTNGTKRFDNVPVLPFNDGVYFASTEKSNIIRGWIFGTTLDSKTQSLLIVNNATNVIKVCEFCQFCNDPFLGVYYHHKNNKSWMESEFRVYSSANNCCTFEVSPQPFMLDEKGKGQGNFKNLREFVFKNIDGYFKYKSHTPINLVRDLPQGSALEPLVLDLPIGINITRFQTLLAHLHSYLTPOSSCGWITAGAAAAYVGYLQPRFTFLKYNNENGTTDAVDACDPLPSETKCTLSFTVEKGIVYOTSFRVQPTESVRFPNITNLCPGEVFNATRFASVYAWNKRISNCVADYSVLYNSASFSTFKCYGVSPTKLNRLCFTNVYADSFVIRGVDEVRQIAQPGQTCGKSTNLVKNCVNFNGLTGTGVLTESNKKFLPFQGFRDIADTTDAVRDPOTLEIDLITPCSGFGSVVITPGNTTSNOVAVLYQGVNCTEVPAVIAHADOLTPTWRYSTGSNTVQTRAGCLIGAEVNNSYEDIPIGACISYQTQNSRRARSVASQSIAYTMSLGAENSVASNNSIAIPNTFTISVTEILPVSMTTKSVDCTMYICGDSTECNLLOYSGFCTQLNRLALTGIAVEQDKNTQEFAQVKQINCKTPPKDFGGFNSQDLPSPSKRSFIEDLFLNKVTLADAGFKIYQGDCGLDIAARDLICAQKFNGLTVLPPLTDEMIAQYTSALAGITTSQTYTQQLRRAEIRASANLAATKMSCEVLGQSKRVDFCGKGYHLMSPQSAHPGVFLHVTVPAQEKNFTTAPACHDGKAHFREGVVFVSGNTHWFTQRNFYEPQIITTDNTFVSGNCDDVIVNNNTVYDPLQPELDSFKEELDKYFKNHTSPDVLDGDISGINASVNIKEIDRNEAKNLNESLIDLQELGKYEQYIKWPWYIWLGFIAGLIAVMVIMLCMTSCSCLKGCCSCGCKFSCFKFEDDSEPVLKGVKLHY*	G75V, T76I, RSYLTGD246-253N, I452Q, F490S, D614G, T859N
B.1.621 (Mu)	MFVFVLLPLVSSQCVNLRTTQLPAPPNTSFRGVVYYPDKVFRSSVLHSTQDLFLPFFSNVTWFHAIHVGSTNGTKRFDNVPVLPFNDGVYFASTEKSNIIRGWIFGTTLDSKTQSLLIVNNATNVIKVCEFCQFCNDPFLGVYYHHKNNKSWMESEFRVYSSANNCCTFEVSPQPFMLDEKGKGQGNFKNLREFVFKNIDGYFKYKSHTPINLVRDLPQGSALEPLVLDLPIGINITRFQTLLAHLHSYLTPOSSCGWITAGAAAAYVGYLQPRFTFLKYNNENGTTDAVDACDPLPSETKCTLSFTVEKGIVYOTSFRVQPTESVRFPNITNLCPGEVFNATRFASVYAWNKRISNCVADYSVLYNSASFSTFKCYGVSDSSCGWITAGAAAAYVGYLQPRFTFLKYNNENGTTDAVDACDPLPSETKCTLSFTVEKGIVYOTSFRVQPTESVRFPNITNLCPGEVFNATRFASVYAWNKRISNCVADYSVLYNSASFSTFKCYGVSPTKLNRLCFTNVYADSFVIRGVDEVRQIAQPGQTCGKSTNLVKNCVNFNGLTGTGVLTESNKKFLPFQGFRDIADTTDAVRDPOTLEIDLITPCSGFGSVVITPGNTTSNOVAVLYQGVNCTEVPAVIAHADOLTPTWRYSTGSNTVQTRAGCLIGAEVNNSYEDIPIGACISYQTQNSRRARSVASQSIAYTMSLGAENSVASNNSIAIPNTFTISVTEILPVSMTTKSVDCTMYICGDSTECNLLOYSGFCTQLNRLALTGIAVEQDKNTQEFAQVKQINCKTPPKDFGGFNSQDLPSPSKRSFIEDLFLNKVTLADAGFKIYQGDCGLDIAARDLICAQKFNGLTVLPPLTDEMIAQYTSALAGITTSQTYTQQLRRAEIRASANLAATKMSCEVLGQSKRVDFCGKGYHLMSPQSAHPGVFLHVTVPAQEKNFTTAPACHDGKAHFREGVVFVSGNTHWFTQRNFYEPQIITTDNTFVSGNCDDVIVNNNTVYDPLQPELDSFKEELDKYFKNHTSPDVLDGDISGINASVNIKEIDRNEAKNLNESLIDLQELGKYEQYIKWPWYIWLGFIAGLIAVMVIMLCMTSCSCLKGCCSCGCKFSCFKFEDDSEPVLKGVKLHY*	T95I, Y145S, Y145N, R346K, E484K, N501Y, D614G, P681H, D950N
B.1.1.529 (Omicron)	MFVFVLLPLVSSQCVNLRTTQLPAPPNTSFRGVVYYPDKVFRSSVLHSTQDLFLPFFSNVTWFHISGTINGTKRFDNVPVLPFNDGVYFASTEKSNIIRGWIFGTTLDSKTQSLLIVNNATNVVIKVCFOFCNDPFLDHKNNKSWMESEFRVYSSANNCCTFEVSPQPFMLDEKGKGQGNFKNLREFVFKNIDGYFKYKSHTPINLVRDLPQGSALEPLVLDLPIGINITRFQTLLAHLHSYLTPOSSCGWITAGAAAAYVGYLQPRFTFLKYNNENGTTDAVDACDPLPSETKCTLSFTVEKGIVYOTSFRVQPTESVRFPNITNLCPGEVFNATRFASVYAWNKRISNCVADYSVLYNSASFSTFKCYGVSPSPKTLNRLCFTNVYADSFVIRGVDEVRQIAQPGQTCGKSTNLVKNCVNFNGLTGTGVLTESNKKFLPFQGFRDIADTTDAVRDPOTLEIDLITPCSGFGSVVITPGNTTSNOVAVLYQGVNCTEVPAVIAHADOLTPTWRYSTGSNTVQTRAGCLIGAEVNNSYEDIPIGACISYQTQNSRRARSVASQSIAYTMSLGAENSVASNNSIAIPNTFTISVTEILPVSMTTKSVDCTMYICGDSTECNLLOYSGFCTQLNRLALTGIAVEQDKNTQEFAQVKQINCKTPPKDFGGFNSQDLPSPSKRSFIEDLFLNKVTLADAGFKIYQGDCGLDIAARDLICAQKFNGLTVLPPLTDEMIAQYTSALAGITTSQTYTQQLRRAEIRASANLAATKMSCEVLGQSKRVDFCGKGYHLMSPQSAHPGVFLHVTVPAQEKNFTTAPACHDGKAHFREGVVFVSGNTHWFTQRNFYEPQIITTDNTFVSGNCDDVIVNNNTVYDPLQPELDSFKEELDKYFKNHTSPDVLDGDISGINASVNIKEIDRNEAKNLNESLIDLQELGKYEQYIKWPWYIWLGFIAGLIAVMVIMLCMTSCSCLKGCCSCGCKFSCFKFEDDSEPVLKGVKLHY*	A67V, del69-70, T95I, G142D/del143-145, del211/L212I, Ins214EPE, G339D, S371L, S373P, S375F, S375F, K417N, N440K, G446S, S477N, T478K, E484A, Q493R, G496S, Q498R, N501Y, Y505H, T547K, D614G, H655Y, N679K, P681H, N764K, D796Y, N856K, Q954H, N969K, L981F
Omicron BA.1	MFVFVLLPLVSSQCVNLRTTQLPAPPNTSFRGVVYYPDKVFRSSVLHSTQDLFLPFFSNVTWFHISGTINGTKRFDNVPVLPFNDGVYFASTEKSNIIRGWIFGTTLDSKTQSLLIVNNATNVVIKVCFOFCNDPFLDVYHHKNNKSWMESEFRVYSSANNCCTFEVSPQPFMLDEKGKGQGNFKNLREFVFKNIDGYFKYKSHTPINLVRDLPQGSALEPLVLDLPIGINITRFQTLLAHLHSYLTPOSSCGWITAGAAAAYVGYLQPRFTFLKYNNENGTTDAVDACDPLPSETKCTLSFTVEKGIVYOTSFRVQPTESVRFPNITNLCPGEVFNATRFASVYAWNKRISNCVADYSVLYNSASFSTFKCYGVSPYRVLSELSELLHAPATVCGPKKSTNLVKNCVNFNGLTGTGVLTESNKKFLPFQGFRDIADTTDAVRDPOTLEIDLITPCSGFGSVVITPGNTTSNOVAVLYQGVNCTEVPAVIAHADOLTPTWRYSTGSNTVQTRAGCLIGAEVNNSYEDIPIGACISYQTQNSRRARSVASQSIAYTMSLGAENSVASNNSIAIPNTFTISVTEILPVSMTTKSVDCTMYICGDSTECNLLOYSGFCTQLNRLALTGIAVEQDKNTQEFAQVKQINCKTPPKDFGGFNSQDLPSPSKRSFIEDLFLNKVTLADAGFKIYQGDCGLDIAARDLICAQKFNGLTVLPPLTDEMIAQYTSALAGITTSQTYTQQLRRAEIRASANLAATKMSCEVLGQSKRVDFCGKGYHLMSPQSAHPGVFLHVTVPAQEKNFTTAPACHDGKAHFREGVVFVSGNTHWFTQRNFYEPQIITTDNTFVSGNCDDVIVNNNTVYDPLQPELDSFKEELDKYFKNHTSPDVLDGDISGINASVNIKEIDRNEAKNLNESLIDLQELGKYEQYIKWPWYIWLGFIAGLIAVMVIMLCMTSCSCLKGCCSCGCKFSCFKFEDDSEPVLKGVKLHY*	A67V, del69-70, T95I, G142D/del143-145, del211/L212I, G339D, S371L, S373P, S375F, S477N, T478K, E484A, Q493R, G496S, Q498R, N501Y, Y505H, T547K, D614G, H655Y, N679K, P681H, N764K, D796Y, N856K, Q954H, N969K, L981F
Omicron BA.2	MFVFVLLPLVSSQCVNLRTTQLPAPPNTSFRGVVYYPDKVFRSSVLHSTQDLFLPFFSNVTWFHAIHVGSTNGTKRFDNVPVLPFNDGVYFASTEKSNIIRGWIFGTTLDSKTQSLLIVNNATNVVIKVCFOFCNDPFLDVYHHKNNKSWMESEFRVYSSANNCCTFEVSPQPFMLDEKGKGQGNFKNLREFVFKNIDGYFKYKSHTPINLVRDLPQGSALEPLVLDLPIGINITRFQTLLAHLHSYLTPOSSCGWITAGAAAAYVGYLQPRFTFLKYNNENGTTDAVDACDPLPSETKCTLSFTVEKGIVYOTSFRVQPTESVRFPNITNLCPGEVFNATRFASVYAWNKRISNCVADYSVLYNSASFSTFKCYGVSSGWTAGAAAYVGYLQPRFTFLKYNNENGTTDAVDACDPLPSETKCTLSFTVEKGIVYOTSFRVQPTESVRFPNITNLCPGEVFNATRFASVYAWNKRISNCVADYSVLYNSASFSTFKCYGVPSGPYRVLSELSELLHAPATVCGPKKSTNLVKNCVNFNGLTGTGVLTESNKKFLPFQGFRDIADTTDAVRDPOTLEIDLITPCSGFGSVVITPGNTTSNOVAVLYQGVNCTEVPAVIAHADOLTPTWRYSTGSNTVQTRAGCLIGAEVNNSYEDIPIGACISYQTQNSRRARSVASQSIAYTMSLGAENSVASNNSIAIPNTFTISVTEILPVSMTTKSVDCTMYICGDSTECNLLOYSGFCTQLNRLALTGIAVEQDKNTQEFAQVKQINCKTPPKDFGGFNSQDLPSPSKRSFIEDLFLNKVTLADAGFKIYQGDCGLDIAARDLICAQKFNGLTVLPPLTDEMIAQYTSALAGITTSQTYTQQLRRAEIRASANLAATKMSCEVLGQSKRVDFCGKGYHLMSPQSAHPGVFLHVTVPAQEKNFTTAPACHDGKAHFREGVVFVSGNTHWFTQRNFYEPQIITTDNTFVSGNCDDVIVNNNTVYDPLQPELDSFKEELDKYFKNHTSPDVLDGDISGINASVNIKEIDRNEAKNLNESLIDLQELGKYEQYIKWPWYIWLGFIAGLIAVMVIMLCMTSCSCLKGCCSCGCKFSCFKFEDDSEPVLKGVKLHY*	A67V, del69-70, T95I, G142D/del143-145, del211/L212I, G339D, S371L, S373P, S375F, S477N, T478K, E484A, Q493R, G496S, Q498R, N501Y, Y505H, T547K, D614G, H655Y, N679K, P681H, N764K, D796Y, N856K, Q954H, N969K, L981F
Omicron BA.2.1	MFVFVLLPLVSSQCVNLRTTQLPAPPNTSFRGVVYYPDKVFRSSVLHSTQDLFLPFFSNVTWFHAIHVGSTNGTKRFDNVPVLPFNDGVYFASTEKSNIIRGWIFGTTLDSKTQSLLIVNNATNVVIKVCFOFCNDPFLDVYHHKNNKSWMESEFRVYSSANNCCTFEVSPQPFMLDEKGKGQGNFKNLREFVFKNIDGYFKYKSHTPINLVRDLPQGSALEPLVLDLPIGINITRFQTLLAHLHSYLTPOSSCGWITAGAAAAYVGYLQPRFTFLKYNNENGTTDAVDACDPLPSETKCTLSFTVEKGIVYOTSFRVQPTESVRFPNITNLCPGEVFNATRFASVYAWNKRISNCVADYSVLYNSASFSTFKCYGVSSGWTAGAAAYVGYLQPRFTFLKYNNENGTTDAVDACDPLPSETKCTLSFTVEKGIVYOTSFRVQPTESVRFPNITNLCPGEVFNATRFASVYAWNKRISNCVADYSVLYNSASFSTFKCYGVPSGPYRVLSELSELLHAPATVCGPKKSTNLVKNCVNFNGLTGTGVLTESNKKFLPFQGFRDIADTTDAVRDPOTLEIDLITPCSGFGSVVITPGNTTSNOVAVLYQGVNCTEVPAVIAHADOLTPTWRYSTGSNTVQTRAGCLIGAEVNNSYEDIPIGACISYQTQNSRRARSVASQSIAYTMSLGAENSVASNNSIAIPNTFTISVTEILPVSMTTKSVDCTMYICGDSTECNLLOYSGFCTQLNRLALTGIAVEQDKNTQEFAQVKQINCKTPPKDFGGFNSQDLPSPSKRSFIEDLFLNKVTLADAGFKIYQGDCGLDIAARDLICAQKFNGLTVLPPLTDEMIAQYTSALAGITTSQTYTQQLRRAEIRASANLAATKMSCEVLGQSKRVDFCGKGYHLMSPQSAHPGVFLHVTVPAQEKNFTTAPACHDGKAHFREGVVFVSGNTHWFTQRNFYEPQIITTDNTFVSGNCDDVIVNNNTVYDPLQPELDSFKEELDKYFKNHTSPDVLDGDISGINASVNIKEIDRNEAKNLNESLIDLQELGKYEQYIKWPWYIWLGFIAGLIAVMVIMLCMTSCSCLKGCCSCGCKFSCFKFEDDSEPVLKGVKLHY*	T19I, L24S, del25-27, G142D, V213G, G339D, S371F, S373P, S375F, T376A, D405N, R408S, K417N, N440K, S477N, T478K, E484A, Q493R, Q498R, N501Y, Y505H, D614G, H655Y, N679K, P681H, N764K, D796Y, Q954H, N969K
Omicron BA.2.12.1	MFVFVLLPLVSSQCVNLRTTQLPAPPNTSFRGVVYYPDKVFRSSVLHSTQDLFLPFFSNVTWFHAIHVGSTNGTKRFDNVPVLPFNDGVYFASTEKSNIIRGWIFGTTLDSKTQSLLIVNNATNVVIKVCFOFCNDPFLDVYHHKNNKSWMESEFRVYSSANNCCTFEVSPQPFMLDEKGKGQGNFKNLREFVFKNIDGYFKYKSHTPINLVRDLPQGSALEPLVLDLPIGINITRFQTLLAHLHSYLTPOSSCGWITAGAAAAYVGYLQPRFTFLKYNNENGTTDAVDACDPLPSETKCTLSFTVEKGIVYOTSFRVQPTESVRFPNITNLCPGEVFNATRFASVYAWNKRISNCVADYSVLYNSASFSTFKCYGVSSGWTAGAAAYVGYLQPRFTFLKYNNENGTTDAVDACDPLPSETKCTLSFTVEKGIVYOTSFRVQPTESVRFPNITNLCPGEVFNATRFASVYAWNKRISNCVADYSVLYNSASFSTFKCYGVPSGPYRVLSELSELLHAPATVCGPKKSTNLVKNCVNFNGLTGTGVLTESNKKFLPFQGFRDIADTTDAVRDPOTLEIDLITPCSGFGSVVITPGNTTSNOVAVLYQGVNCTEVPAVIAHADOLTPTWRYSTGSNTVQTRAGCLIGAEVNNSYEDIPIGACISYQTQNSRRARSVASQSIAYTMSLGAENSVASNNSIAIPNTFTISVTEILPVSMTTKSVDCTMYICGDSTECNLLOYSGFCTQLNRLALTGIAVEQDKNTQEFAQVKQINCKTPPKDFGGFNSQDLPSPSKRSFIEDLFLNKVTLADAGFKIYQGDCGLDIAARDLICAQKFNGLTVLPPLTDEMIAQYTSALAGITTSQTYTQQLRRAEIRASANLAATKMSCEVLGQSKRVDFCGKGYHLMSPQSAHPGVFLHVTVPAQEKNFTTAPACHDGKAHFREGVVFVSGNTHWFTQRNFYEPQIITTDNTFVSGNCDDVIVNNNTVYDPLQPELDSFKEELDKYFKNHTSPDVLDGDISGINASVNIKEIDRNEAKNLNESLIDLQELGKYEQYIKWPWYIWLGFIAGLIAVMVIMLCMTSCSCLKGCCSCGCKFSCFKFEDDSEPVLKGVKLHY*	T19I, L24S, del25-27, G142D, V213G, G339D, S371F, S373P, S375F, T376A, D405N, R408S, K417N, N440K, S477N, T478K, E484A, Q493R, Q498R, N501Y, Y505H, D614G, H655Y, N679K, P681H, S704L, N764K, D796Y, Q954H, N969K

Omicron BA.3	<p>MFVFLVLLPVSSQCVNLITRQLPPAYTNSFRGVYYPDKVFSSVLFHISGTNGTKRFDPNVLPFDGVDVFASIEKSNIIRGWIFGTLDSKTQSLLIVNNATNVVIK VCEFOFCNDPFLDHKNKNSWMESEFRVYSSANNCTFEYVSPFPLMDLEGKQGNFKNLREFVKNIDGYFKIHKTPIVRDLPGFSALEPLVDLPIGINTRFQTLLAHRSYLTPGDSSGW TAGAAAAYVGYLOPRTFLLKYNEENGTTDAVDCALDPLSETKCTLKSFTEKGIVYTSNFRVOPTESIVRPNITLCPDEVFENATRFAZYAWNRKRISNCVADSYLYNFAFFFAFKCYGVS PTKLNLDLCFTNVYADSFVRGNEVSQIAGQTCGNIDYNYKLPLDDFTGCVIAWSNKLDSKVSGNLYNLRFKSLNPKFERDISTEYQAGNKPCNGVAGFNCYFPLRSYGFRTYVGHQ PYRIVVLVLSFELLHAPATVCGPKSTNLVKNKCVNFNGLTGVLTESNKKLPQFGRDIADTTDAVRDPOLEIDLTCSFGGVSVITPGTNTSNOAVLYQQVNCTEVPAIHADOLTP TWRVYSTGSNVFQTRAGCLIGAEYVNNSYECDIPAGICASYQTQTKSHRRARSVASQSIIAYTMSLGAENSENVIASIAINTFTSITVTEILPVSMITKTSVDCTMYIGDSTECSNLLQYG SFCCTLKRALTGIAVEODKNTQEVAQVKOIKTPPKYFGFNFNSQJLPPSKPKRSFIEDLFFNKVTLADAGFIQYGDCLGDIARDLCAQKFNGLTVPPLLTDEMAQYTSALLAGTTG WTFGAGAAALQIPFAMQAMAYRFGNGIVGTVNLYENQKLNQFNSAIGKIQDLSLSTASALGKLQDVVNHNQAOLNTVKQLSKFGAISSVNLDSRLDKEAEVQIDRLITGRLOSLQTYVTQ QLIRAAEIRASANLAATKMSCEVLGGSKRDFCGKGYHLMSPQSPASHGVFLHVTVPAQEKENFTTAPICHDGKAHFREGVFSNGTHWFVQRNFYEPQIITTDNTFVSGNCDDVVIGIVN NTVYDPLQPELDSFKEELDKYFKNHTSPDVLDGDISGINASVNVQKEIDRLNEVAKNLNESLIDLQELGKYEQYIKWPWYIWLGFIAGLIAIVMVTIMLCMTSCCSCLKGCCSGCCKFDED SEPVLKGVKLHY*</p>	A67V, del69-70, T95I, G142D, del143-145, del211/L212I, G339D, S371F, S373P, S375F, T376A, D405N, R408S, K417N, N440K, G446S, S477N, T478K, E484A, Q493R, Q498R, N501Y, Y505H, D614G, H655Y, N679K, P681H, N764K, D796Y, Q954H, N969K
Omicron BA.4/5	<p>MFVFLVLLPVSSQCVNLITRQLPPAYTNSFRGVYYPDKVFSSVLFHISGTNGTKRFDPNVLPFDGVDVFASIEKSNIIRGWIFGTLDSKTQSLLIVNNATNVVIK EFOFCNDPFLDVYYHKNKNSWMESEFRVYSSANNCTFEYVSPFPLMDLEGKQGNFKNLREFVKNIDGYFKIHTPINLGRDLPGFSALEPLVDLPIGINTRFQTLLAHRSYLTPGDSS GWTAGAAAAYVGYLOPRTFLLKYNEENGTTDAVDCALDPLSETKCTLKSFTEKGIVYTSNFRVOPTESIVRPNITLCPDEVFENATRFAZYAWNRKRISNCVADSYLYNFAFFFAFKCYG VSPTKLNLDLCFTNVYADSFVRGNEVSQIAPGQTGNIADYNYKLPLDDFTGCVIAWSNKLDSKVGGNLYNRYRFLRKSNLKPFERDISTEYQAGNKPCNGVAGFNCYFPLQSYGFRTYVG HQPYRVVLLSSELLHAPATVCGPKSTNLVKNKCVNFNGLTGVLTESNKKLPQFGRDIADTTDAVRDPOLEIDLTCSFGGVSVITPGTNTSNOAVLYQQVNCTEVPAIHAD LTPTWRVYSTGSNVFQTRAGCLIGAEYVNNSYECDIPAGICASYQTQTKSHRRARSVASQSIAYTMSLGAENSENVIASIAINTFTSITVTEILPVSMITKTSVDCTMYIGDSTECSNLLQ YGSFCCTLKRALTGIAVEODKNTQEVAQVKOIKTPPKYFGFNFNSQJLPPSKPKRSFIEDLFFNKVTLADAGFIQYGDCLGDIARDLCAQKFNGLTVPPLLTDEMAQYTSALLAGTTG SGWTFGAGAAALQIPFAMQAMAYRFGNGIVGTVNLYENQKLNQFNSAIGKIQDLSLSTASALGKLQDVVNHNQAOLNTVKQLSKFGAISSVNLDSRLDKEAEVQIDRLITGRLOSLQTYVTQ QQLIRAAEIRASANLAATKMSCEVLGGSKRDFCGKGYHLMSPQSPASHGVFLHVTVPAQEKENFTTAPICHDGKAHFREGVFSNGTHWFVQRNFYEPQIITTDNTFVSGNCDDVVIGIVN NTVYDPLQPELDSFKEELDKYFKNHTSPDVLDGDISGINASVNVQKEIDRLNEVAKNLNESLIDLQELGKYEQYIKWPWYIWLGFIAGLIAIVMVTIMLCMTSCCSCLKGCCSGCCKFDED SEPVLKGVKLHY*</p>	T19I, L24S, del25-27, del69- 70, G142D, V213G, G339D, S371F, S373P, S375F, T376A, D405N, R408S, K417N, N440K, L452R, S477N, T478K, E484A, F486V, Q498R, N501Y, Y505H, D614G, H655Y, N679K, P681H, N764K, D796Y, Q954H, N969K